Electronic Supplementary Material (ESI) for Photochemical & Photobiological Sciences

Is Photoactive Yellow Protein a UV-B/Blue Light Photoreceptor?

Elizabeth C. Carroll,[1] Marijke Hospes,[2] Carmen Valladares,[1] Klaas J. Hellingwerf,[2] Delmar S. Larsen[1]*

[1]Department of Chemistry, University of California, Davis, One Shields Avenue, Davis CA 95616 USA, [2]Laboratory for Microbiology, Swammerdam Institute for Life Sciences (SILS), BioCentrum, University of Amsterdam, Amsterdam, The Netherlands

Supporting Information

I. Experimental Methods.

Protein expression and purification. Site-directed mutagenesis was performed using the QuickChange kit (Stratagene) and with pHisp as template.[1] The sequences of the mutagenic primers for W119F were: 5` CCGGCGACAGCTACTTCGTCTTCGTCAAGCGC 3` and 5` GCGCTTGACGAAGACGAAGTAGCTGTCGCCGG 3`. The mutation was confirmed by DNA sequencing. Wild type PYP and its W119F mutant derivative were produced and isolated as described previously for wild type PYP.[1] Apo-PYP was reconstituted with the 1,1'-carbonyldiimidazole derivative of *p*-coumaric acid.[2] The reconstituted holo-proteins were purified in two subsequent steps, with Ni-affinity chromatography and anion exchange, respectively.[3] The purified holo-proteins were used without removal of the genetically introduced N-terminal hexa-histidine containing tag. Their purity index, as determined by the ratio A_{280}/ A_{447} was better than 0.5.

Femtosecond transient absorption. Dispersed-probe transient absorption measurements were obtained with a spectrometer based on an amplified Ti:sapphire laser system.[4] A home-built non-collinear optical parametric amplifier (NOPA) produced short pulses that were frequency doubled to produce excitation pulses at 450 nm and 290 nm. In the case of the 450-nm pulses, frequency doubling of 900-nm (idler) pulses was achieved in the same BBO crystal as parametric amplification. In the case of 290-nm pulses, frequency doubling of 580-nm pulses was achieved in a secondary BBO crystal following pulse compression with a fused-silica prism pair. Changes in absorption were monitored with an ultrafast white light continuum (350-650 nm) linearly polarized at magic angle (54.7°) relative to the pump pulse. Buffered PYP samples were diluted to an optical density of ~1 and circulated through a custom 1-mm path length flow cell with 0.5 mm-thick quartz windows. The sample is flowed to replenish the sample between laser shots. The instrument response function was 100 fs for 450 nm pulses and 200 fs for 290 nm pulses. The pulse energy was 50-200 nJ per pulse. The pulse intensities were sufficiently low to avoid multiphoton ionization processes previously observed in PYP under 400-nm excitation.

II. Data Analysis.

Transient absorption data collected in *wt* PYP and W119F PYP under 447-nm excitation and 290-nm excitation were fit globally to first-order rate equation models. The basic model, adapted from Larsen, *et al.*,[5] includes three excited state intermediates (denoted ESI1, ESI2, ESI3) to represent the multi-exponential excited state decay in PYP. Population evolving through these ESI states can branch into either the photochemical pathway that leads to photocycle intermediate I_1 or proceed through a photochemically inactive pathway and return through a ground state intermediate (GSI) before returning to the equilibrated pG ground state within a few ps. The UV excitation model was modified for single-Trp PYP by including a parallel excitation pathway for Trp and adding a FRET decay channel. These models are shown in **Figure S1**. For simplicity, the spectra for ESI1, ESI2, and ESI3 were assumed to be the same and are represented at a single "pCA*" state in the main article. The branching ratio of I_0 was determined by assuming that the loss of amplitude of in the region 375-440 nm between I_0 and I_1 results from population flow from I_0 that fills in the ground state bleach. The time constants obtained from this model are shown in **Table S1**.

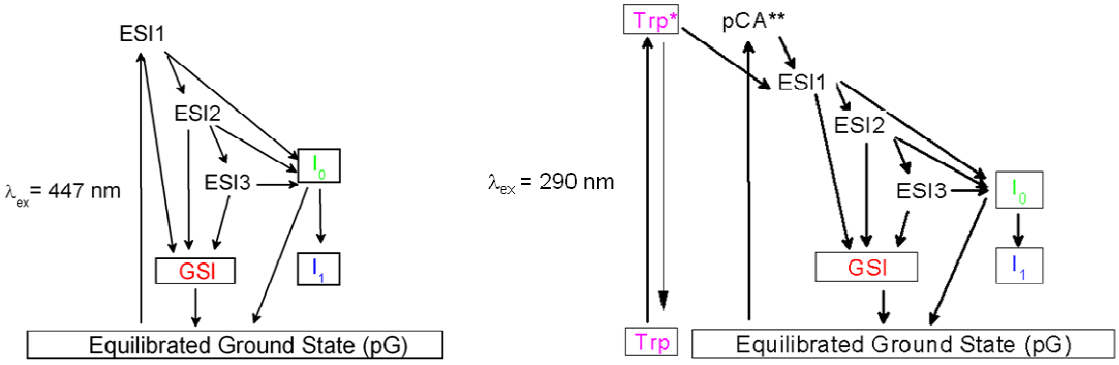

Figure S1. A comparison of the fits obtained to rate equation models for blue (left) and UV excitation (right).

For completeness, we note several variations on the blue excitation model that can describe the transient absorption data equally well. The first model variation is to introduce inhomogeneity explicitly as ESI1, ESI2, ESI3 populations independently excited by the laser pulse. This model is compelling from a physical standpoint because the three ESI can be intuitively assigned to different configurations of PYP. This model however, introduces extra fitting parameters in the form of initial ESI populations, and for the sake of simplifying the current analysis, we have modeled the initial population as a "homogenous" ESI1 that sequentially evolves into ESI2 and ESI3 populations. These populations can still be interpreted

as dynamics resulting from differing configurations of PYP (with excitation probabilities related to the rates $k_{ESI1\rightarrow ESI2}$ and $k_{ESI2\rightarrow ESI3}$) or simply sequential non-exponential evolution of a single population.

Table S1. Global analysis parameters.

λ_{ex} (nm)	Sample	State	Excited state Intermediates			GSI	Photocycle Intermediates		RET
			ESI1	ESI2	ESI3		I_0	I_1	
447	WT	Lifetime	700 fs	3.7 ps	30 ps	2.1 ps	900 ps	∞	--
		Branching yields (%)	0.25 (GSB) 0.37 (ESI2) 0.09 (GSI) 0.29 (I_0)	0.17 (ESI3) 0.53 (GSI) 0.30 (I_0)	0.98 (GSI) 0.02 (I_0)	--	0.64 (I_1) 0.36 (GSB)	--	--
	W119F	Lifetime	780 fs	3.8 ps	30 ps	2.1 ps	850 ps	∞	--
		Branching yields (%)	0.18 (GSB) 0.40 (ESI2) 0.08 (GSI) 0.32 (I_0)	0.17 (ESI3) 0.53 (GSI) 0.30 (I_0)	0.98 (GSI) 0.02 (I_0)	--	0.56 (I_1) 0.44 (GSB)	--	--
290	WT	Lifetime	650 fs	2.8 ps	29 ps	2.1 ps	740	∞	180 ps
		Branching yields (%)	0.23 (GSB) 0.40 (ESI2) 0.09 (GSI) 0.28 (I_0)	0.11 (ESI3) 0.65 (GSI) 0.23 (I_0)	0.94 (GSI) 0.06 (I_0)	--	0.67 (I_1) 0.33 (GSB)	--	100
	W119F	Lifetime	660 fs	2.8 ps	30 ps	2.1 ps	740 ps	∞	--
		Branching yields (%)	0.17 (GSB) 0.50 (ESI2) 0.06 (GSI) 0.27 (I_0)	0.19 (ESI3) 0.66 (GSI) 0.16 (I_0)	0.98 (GSI) 0.02 (I_0)	--	0.67 (I_1) 0.33 (GSB)	--	--

A second point of variation is whether I_0 branches between ground state and I_1 or evolves to I_1 with 100% yield. The choice of model here depends on how one interprets the spectral evolution from I_0 to I_1. Between ~50 ps and 1 ns, the apparent peak of the transient absorption shifts from ~510 nm to ~480 nm, indicating that the absorption peak of I_1 is blue-shifted compared to I_0. ΔA is also uniformly reduced in the region 375-450 nm in this time because the transient spectrum is a combination of GSB and the I_0 and I_1 spectra. But, how much of the ΔA decay is due to GSB recovery and how much is due to I_1 growth? If we assume that the I_0 and I_1 absorption bands are very broad and significantly overlap the ground state bleach (GSB, ~375-500 nm), the increased overlap in the blue-shifted I_1 state would result in reduced ΔA amplitude in the region of the ground state bleach. On the other hand, if we assume that the I_0 and I_1 spectra are relatively narrow and overlap only the red-side of the GSB (440-500 nm), then the only signal contributing to ΔA for $\lambda < 440$ nm is the GSB signal. Then this region of the spectrum

represents a pure loss of ground-state population that can be used to track population refilling the hole in the ground-state population induced by the excitation pulse. Population flow from I_0 that fills in the ground state bleach is introduced to explain the loss of amplitude in the region 375-440 nm. The latter interpretation was used in the present analysis. The branching yields from I_0 and the yield of I_1 are then a result of matching the amplitude of the ground state bleach contribution ($\lambda < 440$ nm) in the SADS representing I_0 and I_1.

We note that the time constants and SADS do not differ significantly if molecules unsuccessful in generating I_1 from I_0 proceed through GSI rather than directly to the equilibrated pG ground state as shown in the original model.[5] As the focus of the present work is in comparing photocycle dynamics between *wt* PYP and the W119F mutant, we consider these variations of the model to be of secondary importance to maintaining self-consistency between the models for UV-B and blue excitation.

To show that global analysis is necessary to determine the quantum yield, we invoke a common alternative method to estimate photocycle yields by the amount of bleach decay that occurs in formation of the I_1 intermediate (**Figure S3**). We assume that the population is entirely in the I_1 intermediate at 6.8 ns, the last time point measured, and estimate the remaining bleach by fitting the ground state absorbance spectrum to the transient spectrum. Because the overlapping I_1 absorption, the peak of the apparent bleach appears blue-shifted from the ground state spectrum, so the fit is based on $\lambda < 440$ nm, where, as noted above, we assume that I_1 does not absorb. The initially excited PYP population was determined by fitting the PYP ground state absorbance spectrum to the transient spectrum at the time of maximum bleach value ("t=0"). Due to overlapping excited state absorption at $\lambda < 450$ nm and stimulated emission at $\lambda > 470$, the fit is based on the range 450-465 nm. Because the time resolution for the UV excitation pulse is poorer, this point occurs at 600 fs, rather than 300 fs as in the blue-excited data. To show that the higher esphotocycle yield in *wt* PYP excited at 290 nm is not an artifact of poorer time resolution (and an underestimation of initially excited PYP population), the 600-fs transient spectrum in *wt* PYP excited at 447 nm is also shown for comparison.

This method would predict a photocycle quantum yield of ~ 0.4 in *wt* PYP excited at 290 nm. However, this would neglect photons absorbed by Trp119, the estimate is far too high.

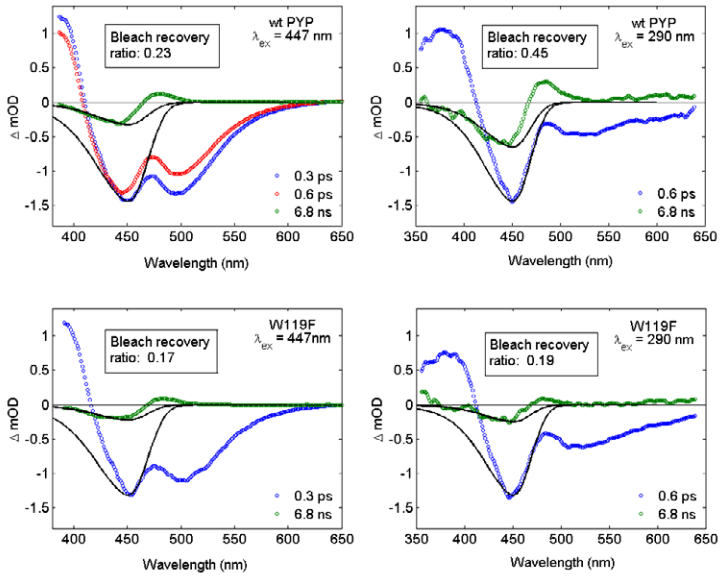

Figure S2. The blue-excited I_1 quantum yield in PYP can be approximated directly from the ground state bleach recovery. The black line in each panel corresponds to the inverted ground state absorption of PYP, scaled to the size of the ground state bleach contribution in the transient spectrum. This method overestimates the

III. Comparison with of FRET rates from protein structures.

The rate of resonant energy transfer between the single Trp residue and pCA was calculated using Förster's equation (**Eq. S1**):

(Eq. S1)
$$k_T = (8.71 \times 10^{23}) \left(\frac{J k^2}{n^4 R_{DA}^6}\right) \left(\frac{\Phi_D}{\tau_D}\right) s^{-1},$$

where J is the spectral overlap integral between the emission spectrum of the donor and the absorption spectrum of the acceptor, k^2 is the angular factor of the interaction between the transition dipole moment of the donor $(\vec{\mu}_D)$ and acceptor $(\vec{\mu}_A)$, and n is the index of refraction. R_{DA} is the distance between the transitional dipole moments of donor and acceptor, τ_D is the fluorescence lifetime of the donor in the absence of the acceptor, and Φ_D is the fluorescence quantum yield of the donor in the absence of the acceptor. All values are based on PYP structures obtained from the Protein Data Bank. The L_a transition dipole moment of tryptophan, based on molecular orbital calculations by Callis, *et al.*[6] while the transition dipole moment of pCA was calculated as a vector connecting the extrema of the conjugated system.[7] The distance

between donor and acceptor is measured from center of each transition dipole. The angular factor was calculated according to Eq S2, where the angles α, β and δ are defined in **Figure S3**. All values are tabulated in **Table S2.**

(Eq. S2)

$$k^2 = (\cos\beta - 3\cos\alpha\cos\delta)^2$$

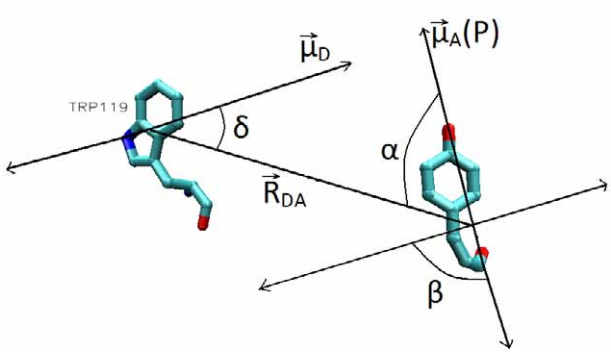

Figure S3. The geometric model used to calculate FRET rate in PYP.

The rate of FRET relies on an accurate calculation of spectral overlap integral between donor emission and acceptor absorption. Tryptophan emission is known to be highly sensitive to environment and the peak of the emission spectrum can change up to 50 nm. In calculating J, we used the tryptophan emission spectrum in water,[8] and adjusted the peak wavelength of emission to match the measured tryptophan emission spectrum from PYP at pH 8.0. The absorption spectrum of *p*-coumaric acid in PYP at pH 8.0 was determined by deconstructing the PYP spectrum in constitute components: pCA, 1×Trp, and 5×Tyrosine. The absorption spectra of the amino acids were obtained from Ref [8].

FRET rates from tryptophan residues to internal cofactors were also calculated in several LOV domains from phototropins and YtvA. The transition dipole moment of FMN was taken along the z-axis. Because, in Eq. S1, it is necessary to know the lifetime of the donor in the absence of the acceptor, the appropriate value to use is the tryptophan fluorescence lifetime in the apo-protein. In apo-protein, the tryptophan fluorescence in the protein will generally be quenched by interactions with other amino acids, in addition to any FRET interactions with cofactors. These values have not been published, so the rates in Table SI3 were calculated using the fluorescence lifetime of tryptophan in water (~5 ns). This overestimated lifetime value will result in a lower limit on the FRET rate. It is worthwhile to note that, like in the PYPs, a dominate factor in the very rapid FRET rate constants is the orientational factor with the

chromophore, which is considerably larger than the 0.66 value assumed by isotropically orientated molecules.

Table S2. FRET parameters calculated from PYPs using Trp119 as the donor and pCA as the acceptor. Other parameters: n = 1.39, τ_D = 4.8 ns, Φ_D = 0.13. Errors are indicated in parentheses.

Protein	Species	PDB	Trp	R_{DA} (Å)	α (deg)	β (deg)	δ (deg)	κ^2	J x 10^{-15} (cm^3 M^{-1})	R_O (Å)	E	k^{-1}_{FRET} (ps)
PYP, pG, crystal[†]	*Halorhodospira halophila*	several[†]	119	16.4 (0.1)	140 (1)	104 (1)	36 (1)	2.60 (0.03)	6.38	27.9 (0.1)	0.96 (0.01)	185 (10)
PYP, pG, solution[‡]	*Halorhodospira halophila*	3PHY[9]	119	15.5 (0.6)	121 (7)	82 (8)	39 (3)	1.8 (0.3)	6.38	26.2 (0.8)	0.96 (0.02)	210 (90)
PYP, pB, crystal	*Halorhodospira halophila*	1TS0[10]	119	18.8	88.9	54.9	33.9	0.28	12.7[7]	21.6	0.69	2000
PYP domain of Ppr	*Rhodospirillum centenum*	1MZU[11]	119	16.2	138	110	27.7	2.64	7.45[*]	28.7	0.97	145

[†]Error values were determined as the variance of values computed from x-ray crystallography structures 1NWZ, 1TS7, 2PYP, and 1OT9 (model 1).

[‡]Error values on the solution NMR structure were determined as the variance among the 26 structures reported in PDB 3PHY.

[*]Value was calculated assuming the same Trp emission spectrum as for wt PYP. Ppr-PYP extinction coefficient was assumed to be equal to PYP from *H. halophila*, based on previous observations that the extinction coefficients of PYP proteins isolated from different organisms are very similar. The spectrum of Ppr-PYP has maximum absorption at 434 nm.[12]

Table S3. Structural FRET parameters calculated from other PAS domains using unique Trp residue as the donor and FMN as the acceptor. We assume the value: n = 1.39, Φ_D = 0.13, and τ_D = 5.0 ns.[†]

Protein	Species	PDB	Trp	R_{DA} (Å)	α (deg)	β (deg)	γ (deg)	κ^2	J x 10^{-15} (cm^3 M^{-1})	R_O (Å)	E	k^{-1}_{FRET} (ps)
LOV domain of YtvA	*Bacillus subtilis*	2PR5[13]	103	16.3	140	100	40	2.52	10.8[†]	30.7	0.98	106
LOV1 domain of phototropin1	*Arabidopsis thaliana*	2Z6C[14]	275	15.2	151	113	37	2.84	9.54[*]	30.6	0.98	75
LOV1 domain of phototropin2	*Arabidopsis thaliana*	2Z6D[14]	211	15.4	152	123	29	3.14	9.54[*]	31.2	0.98	75
LOV2 domain of phototropin	*Avena Sativa*	2V1A[15]	491	15.4	152	111	40	2.72	9.54[*]	30.4	0.98	85
LOV2 domain of PHY3 phototropin	*Adiantum Capillus-Veneris*	1G28[16]	1007	15.3	151	115	36	2.88	9.54[*]	30.7	0.98	80
Phot-LOV1	*Chlamydomonas Reinhardtii*	1N9L[17]	98	15.3	153	110	43	2.62	9.54[*]	30.2	0.98	85

[†]Spectral overlap based on measured YtvA absorption spectrum (ε_{450} ~13000 $M^{-1}cm^{-1}$) and tryptophan emission spectrum in YtvA.[18]

[*]Spectral overlap calculations based on absorption spectrum of LOV2 from *Avena Sativa* and the tryptophan emission spectrum from YtvA.

References

(1) Kort, R.; Hoff, W. D.; VanWest, M.; Kroon, A. R.; Hoffer, S. M.; Vlieg, K. H.; Crielaard, W.; VanBeeumen, J. J.; Hellingwerf, K. J. *Embo J.* **1996**, *15*, 3209-3218.

(2) Hendriks, J.; Gensch, T.; Hviid, L.; van der Horst, M. A.; Hellingwerf, K. J.; van Thor, J. J. *Biophys. J.* **2002**, *82*, 1632-1643.

(3) Hendriks, J., University of Amsterdam, 2002.

(4) Carroll, E. C.; Compton, O. C.; Madsen, D.; Osterloh, F. E.; Larsen, D. S. *Journal of Physical Chemistry C* **2008**, *112*, 2394-2403.

(5) Larsen, D. S.; van Stokkum, I. H. M.; Vengris, M.; van der Horst, M.; de Weerd, F. L.; Hellingwerf, K.; van Grondelle, R. *Biophysical Journal* **2004**, *87*, 1858-1872.

(6) Callis, P. R. *Journal of Chemical Physics* **1991**, *95*, 4230-4240.

(7) Hoersch, D.; Otto, H.; Cusanovich, M. A.; Heyn, M. P. *J. Phys. Chem. B* **2008**, *112*, 9118-9125.

(8) H. Du, R. A. F., J. Li, A. Corkan, J. S. Lindsey *Photochem. Photobiol.* **1998**, *68*, 141-142.

(9) Dux, P.; Rubinstenn, G.; Vuister, G. W.; Boelens, R.; Mulder, F. A.; Hard, K.; Hoff, W. D.; Kroon, A. R.; Crielaard, W.; Hellingwerf, K. J.; Kaptein, R. *Biochemistry* **1998**, *37*, 12689-99.

(10) Ihee, H.; Rajagopal, S.; Srajer, V.; Pahl, R.; Anderson, S.; Schmidt, M.; Schotte, F.; Anfinrud, P. A.; Wulff, M.; Moffat, K. *Proceedings of the National Academy of Sciences of the United States of America* **2005**, *102*, 7145-7150.

(11) Rajagopal, S.; Moffat, K. *Proc. Natl. Acad. Sci.* **2003**, *100*, 1649-1654.

(12) Kyndt, J. A.; Fitch, J. C.; Meyer, T. E.; Cusanovich, M. A. *Biochemistry* **2007**, *46*, 8256-8262.

(13) Moglich, A.; Moffat, K. *Journal of Molecular Biology* **2007**, *373*, 112-126.

(14) Nakasako, M.; Zikihara, K.; Matsuoka, D.; Katsura, H.; Tokutomi, S. *Journal of Molecular Biology* **2008**, *381*, 718-733.

(15) Halavaty, A. S.; Moffat, K. *Biochemistry* **2007**, *46*, 14001-14009.

(16) Crosson, S.; Moffat, K. *Proc. Natl. Acad. Sci.* **2001**, *98*, 2995-3000.

(17) Fedorov, R.; Schlichting, I.; Hartmann, E.; Domratcheva, T.; Fuhrmann, M.; Hegemann, P. *Biophys. J.* **2003**, *84*, 2474-2482.

(18) Losi, A.; Ternelli, E.; Gartner, W. *Photochem. Photobiol.* **2004**, *80*, 150-153.